Journal of Natural Fibers

ISSN: (Print) (Online) Journal homepage: https://www.tandfonline.com/loi/wjnf20

Plant Waste as Green Reinforcement for Polymer Composites: A Case Study of Pteris Vittata Roots

Irene Bavasso, Davide Marzi, Maria Paola Bracciale, Luca Di Palma, Jacopo Tirillò & Fabrizio Sarasini

To cite this article: Irene Bavasso, Davide Marzi, Maria Paola Bracciale, Luca Di Palma, Jacopo Tirillò & Fabrizio Sarasini (2023) Plant Waste as Green Reinforcement for Polymer Composites: A Case Study of Pteris Vittata Roots, Journal of Natural Fibers, 20:1, 2135669, DOI: 10.1080/15440478.2022.2135669

To link to this article: https://doi.org/10.1080/15440478.2022.2135669

JOURNAL OF NATURAL FIBERS
2023, VOL. 20, NO. 1, 2135669
https://doi.org/10.1080/15440478.2022.2135669

Plant Waste as Green Reinforcement for Polymer Composites: A Case Study of Pteris Vittata Roots

Irene Bavasso[a], Davide Marzi[b], Maria Paola Bracciale[a], Luca Di Palma[a], Jacopo Tirillò[a], and Fabrizio Sarasini[a]

[a]Department of Chemical Engineering Materials Environment & UdR INSTM, Sapienza-Università di Roma, Roma, Italy; [b]Department of Biology and Biotechnology "Charles Darwin", Sapienza University of Rome, Rome, Italy

ABSTRACT

Pteris vittata is a hyperaccumulator fern able to uptake arsenic by roots accumulating it in the fronds. Recent studies showed that *Pteris vittata* can be used efficiently for arsenic-contaminated water treatment, paving the way for long-lasting decontamination strategies established on nature-based solutions. This raises the issue of biomass disposal, which rather than being incinerated could represent a valuable untapped source of fibers for sustainable and higher-value biocomposites. Here, *Pteris vittata* waste roots were collected and used to develop composites based on high-density polyethylene. Composites with two amounts of filler (10 wt.% and 20 wt.%) added with 5 wt.% of maleic anhydride grafted polyethylene, were manufactured and tested in terms of mechanical and thermal properties. Mechanical property analysis showed that, compared to neat high-density polyethylene, composites at 20 wt.% filler content with coupling agent displayed an increase around 54% in tensile strength, 100% in Young's modulus, 46% in flexural strength and 45% in flexural modulus. These results demonstrate the potential of *Pteris vittata* waste roots application for sustainable composite materials production.

摘要

虎尾蕨是一种超积累蕨类植物, 能够通过根部在复叶中积累砷来吸收砷. 最近的研究表明, 虎尾蕨可以有效地用于砷污染的水处理, 为基于自然溶液的长期净化策略铺平了道路. 这就提出了生物质处置的问题, 而不是被焚烧, 这可能是一种有价值的未开发纤维来源, 用于可持续和更高价值的生物复合材料. 在这里, 收集虎尾蕨废根, 并用于开发基于高密度聚乙烯的复合材料. 制造了含有两种填料（10 wt.%和20 wt.%）的复合材料, 其中添加了5 wt.%的马来酸酐接枝聚乙烯, 并对其力学性能和热性能进行了测试. 力学性能分析表明, 与纯高密度聚乙烯相比, 填充物含量为20%的偶联剂复合材料的拉伸强度增加了约54%, 杨氏模量增加了100%, 弯曲强度增加了46%, 弯曲模量增加了45%. 这些结果表明, 虎尾蕨废根应用于可持续复合材料生产的潜力.

KEYWORDS

Biocomposites; *Pteris vittata*; polymer-matrix composites; waste reuse; mechanical properties; thermal properties

关键词

生物复合材料; 维塔塔凤蝶; 聚合物基复合材料; 废物再利用; 机械性能; 热性能

Introduction

Heavy metals (HM) pollution is considered one of the most important issues related to anthropogenic activities. The persistence of such contaminants affects environment and human health because of their mutagenic and carcinogenic effects even at low concentrations (Hamilton et al. 1998; Verma et al. 2022). Among different techniques adopted for HM decontamination, phytoremediation takes advantage of plants ability to uptake high amounts of contaminants and represents a sustainable strategy as it is a low-cost and flexible technology (Pilon-Smits 2005). Several studies demonstrated the great

CONTACT Irene Bavasso irene.bavasso@uniroma1.it Department of Chemical Engineering Materials Environment & UdR INSTM, Sapienza-Università di Roma, Via Eudossiana 18, Roma 00184, Italy

potential of the Chinese brake fern *Pteris vittata* (PV) for remediating soil contaminated by Arsenic (As) (Antenozio et al. 2021; Fayiga et al. 2005; Gonzaga, Santos, and Ma 2008; Ma et al. 2001; Zhang et al. 2002; Zhao, Dunham, and McGrath 2002), a carcinogenic metalloid ubiquitously distributed in the environment. It was shown that PV can efficiently remove As from water when grown in hydroponic culture system, suggesting that this approach could be used for drinking water decontamination (Huang et al. 2004; Marzi et al. 2021; Natarajan et al. 2011). In addition, the efficiency of As uptake increases in subsequent phytofiltration cycles, paving the way for long-lasting decontamination strategies. One of the limiting aspects of phytoremediation is the disposal of contaminated waste biomass, which is generally burned out. Because of its lignocellulosic nature (Carrier et al. 2012), such waste can be used as reinforcing agent for wood-plastic composites (WPCs) production. WPCs are biocomposites based on formulations of lignocellulosic-thermoplastic materials and manufactured by techniques such as extrusion, injection and compression molding (Mu et al. 2021). Among the thermoplastic materials, High-Density Polyethylene (HDPE) exhibits excellent characteristics such as lightweight, low cost, chemical-resistance, high impact resistance (Sewda and Maiti 2013) which make HDPE ideal for several applications (electrical power, fiber-optic cables, toys, chemical and pipe devices) (Rasib, Mariatti, and Atay 2021). The addition of a lignocellulosic filler can contribute to ameliorate mechanical properties of the resulting biocomposites. Koffi and collaborators investigated birch fiber/HDPE composites and observed that the addition of up to 40 wt.% of wood filler along with a coupling agent, produced an improvement of the elastic modulus (27.2%) and tensile strength (19.7%) compared to the neat polymer, and a reduction in ductility with the increase of fiber content (Koffi, Koffi, and Toubal 2021). Mu et al. evaluated Moso bamboo fiber (MB) as filler, which proved to be more effective in enhancing tensile and flexural properties of HDPE (tensile and flexural moduli equal to 4.74 GPa and 5.45 GPa, respectively) because of the high lignin and cellulose content (Mu et al. 2021). Vázquez Fletes and Rodrigue tested recycled HDPE composites with maple fiber as filler and with the addition of maleic anhydride grafted polyethylene (MAPE) as coupling agent (CA). The presence of the waste material (45 wt.%) caused an increase in tensile modulus (23%) and strength (26%) and an enhancement of about 54% in flexural modulus (Fletes and Rodrigue 2021). Biocomposites based on 30 wt.% of *Centella asiatica L.* plant and HDPE matrix showed good mechanical properties and an increase in the tensile modulus of about 64% with respect to the neat polymer (Syed and Syed 2016). Barman et al. used *Saccharum spontaneum* grass for the production of HDPE-based composite materials with the addition of a compatibilizer, and the tensile strength and elastic modulus increased by about 13.5% and 57.8% (Barman et al. 2015). The objective of the present paper is to explore the possibility of reusing PV waste roots to produce HDPE-based biocomposites as an additional strategy to biomass valorization (Mazzeo et al. 2022). To the best of authors' knowledge, this is the first time that such biomass waste has been investigated as a potential filler in polymer composites. The biocomposites were prepared by coupling extrusion and injection molding techniques and different formulations were tested, in terms of PV amount and presence of a commercial compatibilizing agent specifically added to counteract the well-known interfacial incompatibility between hydrophobic polyolefins and hydrophilic lignocellulosic fillers (Bartos et al. 2021; Gholampour and Ozbakkaloglu 2020). A detailed description of the thermal, mechanical, and morphological properties of the composites is reported. It is worth noting that currently the Chinese brake fern is widely naturalized in many areas with a mild climate, as it is versatile, fast growing, and perennial with preference for sunny and alkaline environments (Ma et al. 2001). No data are available on its worldwide commercial accessibility, but one can consider the increasing trend in the global scenario of arsenic contamination. To provide some figures, it has been estimated that nearly 108 countries are affected by arsenic contamination in groundwater (with concentration beyond maximum permissible limit of 10 ppb recommended by the World Health Organization) (Shaji et al. 2021). This means that PV, due to its the ability of As hyperaccumulation from the soil, is considered extremely important in phytoremediation, and hence is receiving significant attention (Danh et al. 2014; Vandana et al. 2020). With its increasing use as heavy metals hyperaccumulator (An et al. 2006),

the amount of waste biomass will increase thus making it available in large amount which needs to be considered and treated.

The manuscript is organized as follows. At first the materials and the composite manufacturing process are described, followed by the characterizations performed on waste root fibers (×RD, FT-IR, TGA) and on resulting composites in terms of mechanical (tensile, bending, impact), thermal (TGA, DSC, and DMA), morphological (SEM), and water absorption tests. Then the results obtained on *Pteris vittata* root fiber and on the material configurations considered in this study are discussed, and finally conclusions are drawn at the end of the manuscript.

Materials and methods

Raw materials

Ferns were propagated and grown in a greenhouse according to Marzi and collaborators (Marzi et al. 2021), with slight modifications. Mature spores of the Chinese brake fern *Pteris vittata* were resuspended in water, sown in pots filled with soil and covered with a plastic wrap. About 8 weeks later, young sporophytes (early-stage ferns) showing at least two fronds (leaves), were moved to individual rockwool cubes and placed in mini-greenhouses for 4–6 weeks. Later, young ferns with 4–6 fronds were moved to net pots filled with expanded clay and placed in 15 L tanks of tap water for hydroponic culture, supplied with an air pump. Each tank hosted 12 ferns and after 4–5 months the roots occupied most of the space in the tank, thus they were pruned and harvested. In Figure 1 are reported the representative images of a young *Pteris vittata*, showing the fronds (leaves), the rhizome and the roots (Figure 1a), the hydroponic culture system (Figure 1b) and the roots after 4–5 months of hydroponic growth (Figure 1c). The ferns were placed back to the hydroponic tank, and all survived to the pruning of the roots, without significant detrimental effects. Waste roots were dried at 80°C for 24 h to remove moisture and then milled into particles in the size range from 2.00 to 1.19 mm.

HDPE type Eraclene MP90 (Eni Polimeri Europa) was used as the matrix for biocomposites production, which was modified by adding 5 wt.% Polybond® 3009 (Addivant Corporation). This is a standard maleic anhydride-modified high-density polyethylene (MAPE) with a high (0.80–1.20%) maleic anhydride content (Melt Flow Rate at 190°C/2.16 kg of 5 g/10 min and density of 0.95 g/cm^3).

Composite processing

The composite materials were prepared using a two-stage process involving extrusion (co-rotating twin-screw extruder, Thermo Scientific Process 11, ThermoFisher Scientific) and injection molding (Haake MiniJet IIPro, Thermo Fisher Scientific). During melt compounding, the following

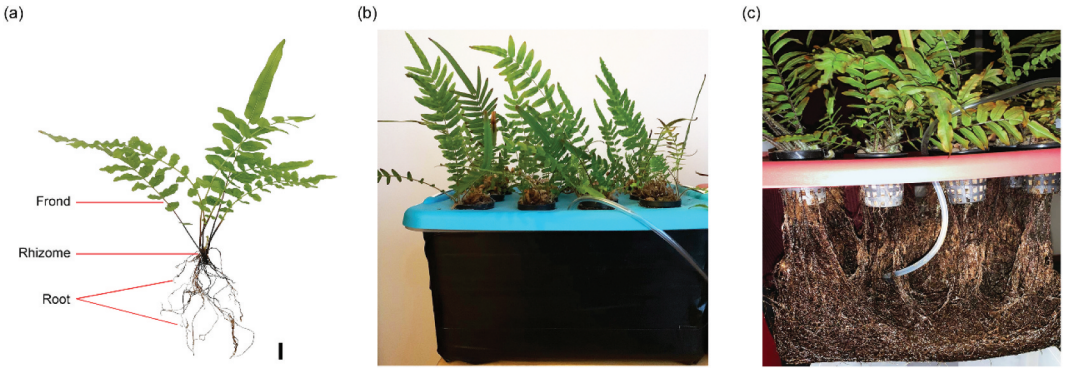

Figure 1. (a) Representative image of a young Pteris (scale bar 1 cm), (b) the hydrophonic cuculturee system used for ferns growth and (c) the roots of the ferns after 4–5 months of hydroponic growth.

Table 1. List of manufactured formulations.

Sample	*Matrix (HDPE) [wt.%]*	*Pteris Vittata (PV) [wt.%]*	*Coupling Agent (POLYBOND 3009) [wt.%]*
HDPE	100	-	-
HDPE_10PV	90	10	-
HDPE_10PV_5CA	85	10	5
HDPE_20PV	80	20	-
HDPE_20PV_5CA	75	20	5

temperature profile from feeder to die was implemented: 160°C—160°C—170°C—180°C—180°C—170°C—170°C—175°C. During the injection, a pressure of 450 bar was maintained for 10 s and a post-injection at 150 bar for additional 10 s was operated. The screw speed was set at 150 rpm, the mold was heated at 35°C while the loading cylinder was kept at 170°C. The different composite formulations are summarized in Table 1.

Experimental characterization

Structural, chemical and thermal assessment of Pteris vittata roor fibers

X-ray diffraction analysis was performed at room temperature on a Philips X'Pert PRO powder diffractometer (CuKα radiation = 1.54060 Å). XRD pattern of powdered PV sample was collected in the range of 2θ = 10° to 50° with a scan step 2θ = 0.02° and a measurement time per step of 4 s at 40 kV and 40 mA.

The chemical composition of the fern waste roots has been studied by Fourier-transform infrared (FT-IR) analysis. Infrared measurements were carried out with a Bruker Vertex 70 spectrometer (Bruker Optik GmbH) equipped with a single reflection Diamond ATR cell. Spectra were recorded with a 3 cm^{-1} spectral resolution in the mid infrared range (400–4000 cm^{-1}) using 512 scans.

Thermogravimetric (TGA) analysis was carried out by heating the powdered PV (around 30 mg) in alumina pan from room temperature to 800°C under nitrogen atmosphere (50 mL/min) and with a heating rate of 10°C/min (Setsys Evolution system by Setaram).

The morphology of *Pteris vittata* fibers was investigated by a scanning electron microscope (FE-SEM Mira3 by Tescan) equipped with an Octane Elect EDS System by EDAX-AMETEK Inc. Fibers were sputter coated with gold before the analysis.

Mechanical properties of HDPE-based composite materials

The tensile and flexural characterizations of composites were carried out on a Zwick/Roell Z010 universal testing machine. Tensile tests were conducted in displacement control with a crosshead speed of 10 mm/min at room temperature according to ISO 527–2 (type 1 BA, l_0 = 30 mm).

Three-point bending tests were performed according to ISO 178. Samples (80 × 10 × 4 mm) were tested at 5 mm/min with a span-to-thickness ratio of 16:1.

Charpy impact tests were carried out in accordance with ISO 179–2 in an edgewise mode. Specimens of 80 × 10 × 4 mm size featured a type A notch, and a span of 62 mm was used. Tests were conducted with a CEAST/Instron 9340 instrumented drop weight tower by using an impact velocity of 2.90 m/s. All tests were repeated at least five times.

Thermal properties of HDPE-based composite materials

Thermogravimetric (TGA) analysis was carried out by heating the samples (around 30 mg) in alumina pan from room temperature to 800°C under nitrogen atmosphere (50 mL/min) and with a heating rate of 10°C/min (Setsys Evolution system by Setaram).

Differential scanning calorimetry (DSC) analysis of the composites was performed with a nitrogen flow of 60 mL/min (DSC 214 Polyma by Netzsch). Specimens (around 10 mg) were placed in a concavus aluminum crucible with pierced lid and analyzed according to the following thermal

program: heating from −40°C to 200°C (5 min hold), cooling to −40°C (5 min hold) and a second heating to 200°C, all steps performed with a rate of 10°C/min. Results as melting and crystallization temperatures and degree of crystallinity ($\times_c$, Equation 1) are reported as mean values of three repetitions:

$$X_C(\%) = \frac{\Delta H_m}{\Delta H_m^0} \frac{100}{(1 - w_f)} \quad (1)$$

where ΔH_m is the experimental enthalpy of melting of the sample (J/g), ΔH_m^0 the enthalpy of melting for 100% crystalline HDPE equal to 293 J/g (Carlson et al. 1998) and w_f is the weight fraction of PV.

The dynamic mechanical analysis (DMA) was employed to measure the composite material properties in the solid state under dynamic conditions as a function of temperature, and the storage (E') and loss moduli (E"), the loss factor (damping parameter), and tanδ (E"/E') were measured. These tests were conducted in a three-point bending mode by using a DMA 242 E Artemis by Netzsch. Samples with size 60 × 10 × 4 mm were subjected to a heating rate of 2°C/min from −160°C up to 100°C at a frequency of 1 Hz.

Water uptake of HDPE-based composites

The water uptake (W_{ut}) of neat HDPE and biocomposites was evaluated by immersion in demineralized water at room temperature in the range of 0–150 h (Kilinc et al. 2016). The W_{ut} (%) was calculated through the Equation 2:

$$W_{ut}(\%) = ([W_w - W_d]/W_d) \times 100 \quad (2)$$

where W_w and W_d represent the weight of specimens in wet and dried conditions, respectively.

Morphological analysis HDPE-based composites

Fracture surface morphologies of composites were studied by means of a scanning electron microscope (FE-SEM Mira3 by Tescan). All specimens were sputter coated with gold before the analysis.

Results and discussion

Characterization of Pteris vittata root fibers

All the ferns survived to the pruning without any significant detrimental effect, highlighting the high resilience of this fern. Indeed, roots were pruned systematically every 4–5 months, showing that this approach is suitable for the management of ferns grown in hydroponic systems. Interestingly, PV accumulates Arsenic mainly in the fronds, while it is found only in traces in the roots due to the fast translocation to the aerial organs (Antenozio et al. 2022; Yamazaki et al. 2008). Thus, to valorize the waste roots derived from the pruning, they were used as reinforcement in high-density polyethylene matrix.

SEM analysis was used to visualize the morphology of PV fiber and results are included in Figure 2. As can be seen from secondary electron micrographs, the PV fiber consisted of quite cylindrical but non-uniform fibers lengthwise, with an average diameter around 193.3 ± 52.10 µm. The surface is not compact and appears to be quite rough and wrinkled, with the presence of a fibrillar structure, similar to the one reported for fibers extracted from the roots of *Acalypha indica L.* plant (Jeyabalaji et al. 2021). These features might be favorable to mechanical interlocking with the matrix during composite manufacturing, while the fibrils might act as an effective reinforcement for composites, as high aspect ratio fibers are known to help distribute the applied load, thus leading to higher mechanical strength (Faludi et al. 2014).

A closer look revealed the presence of particles distributed over the fiber surface, which were analyzed by Energy Dispersive Spectroscopy (EDS). Results included in Figure 3 show that these

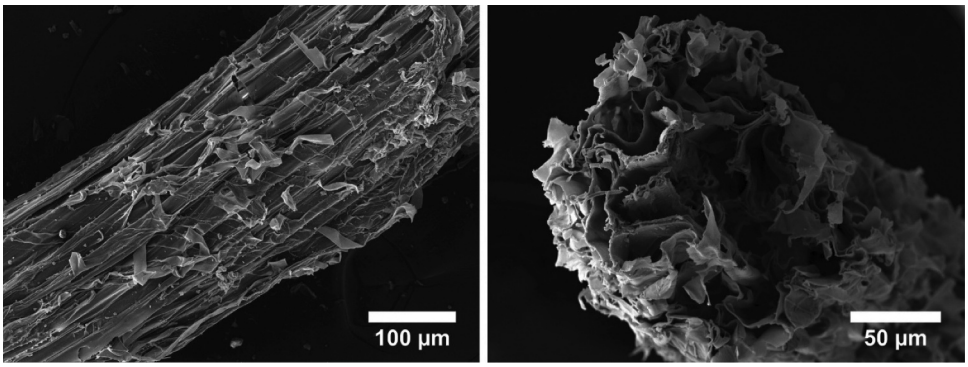

Figure 2. SEM micrographs detailing the surface morphology of as-collected PV root fibers.

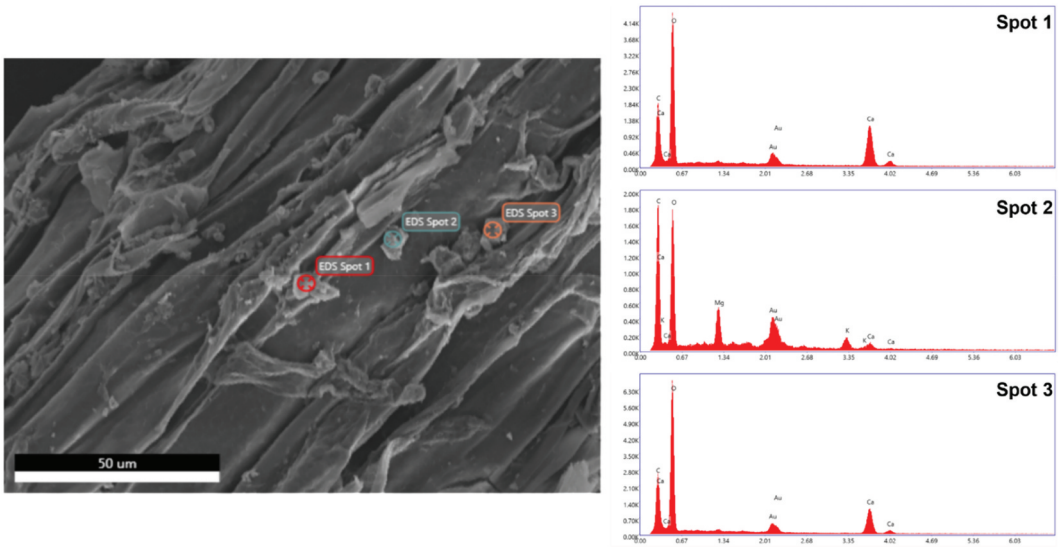

Figure 3. EDS spectra of different spots on the PV fiber surface.

particles are made of elements usually found in tap water, confirming the growth conditions experienced by the PV roots (Marzi et al. 2021).

XRD diffraction analysis supported these results, as can be seen in Figure 4a. In fact, PV fibers exhibited a broad peak centered at $2\theta = 22.6°$ with a shoulder at $2\theta = 15.1–16.6°$, typical of crystallographic form of native cellulose (Tamanna et al. 2021; Yue et al. 2015), but with a low content and crystallization degree, due to the presence of amorphous constituents, namely hemicellulose and lignin, in addition to cellulose that governs the crystallinity of lignocellulosic biomass. Additional peaks in the range 30–50° are all ascribed to calcium carbonate (JCPDS 02–0629), supporting the EDS results. The presence of inorganic particles on the fiber surface resulted also in the occurrence of a significant residue at the end of the thermogravimetric analysis, around 36% (Figure 4b). This is in fact much higher than the one commonly observed for other natural fibers, around 10–20%, depending on the specific fiber (Bourmaud, Morvan, and Baley 2010; Tamanna et al. 2021; Yao et al. 2008).

FT-IR results confirmed the presence of the typical constituents of lignocellulosic fillers (**Figure 5, Table 2**). The functional groups observed in the FT-IR spectrum of the fern sample were assigned to alkenes, esters, alcohol, hydroxyl, and carboxyl belonging to cellulose, hemicellulose, and lignin. The wide band detected at 3300 cm^{-1} corresponded to the intramolecular and intermolecular stretching

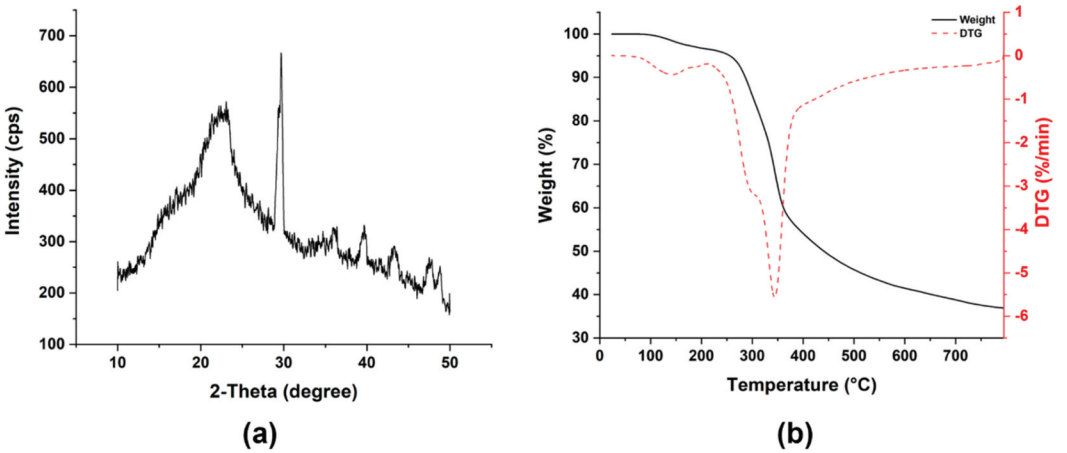

Figure 4. (a) X-ray diffraction pattern of PV root fiber and (b) typical TGA/DTG curves of PV root fiber.

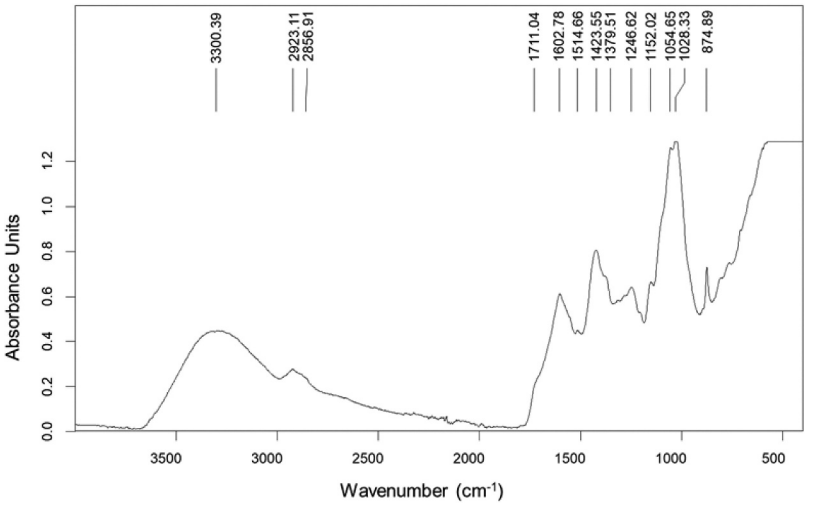

Figure 5. Infrared spectra of PV roots fiber.

Table 2. Assignment of the main ATR-FTIR bands of fern (Xu et al. 2013).

Wavenumber (cm^{-1})	Band Assignments*
3700–3000	νOH
3000–2800	νCH of cellulose and hemicellulose
1711	νC=O of hemicellulose and lignin
1603, 1515	νC=C and dCH in methyl, methylene and methoxyl groups of lignin
1424, 1380	in-plane dCH of lignin and δCH in cellulose and hemicellulose
1247, 1152, 1028	νC-O of polysaccharide components (mainly hemicellulose), νC-O-C in cellulose and hemicellulose, dCH of cellulose and νC-O of hemicellulose
1055	νC-OH of cellulose
875	β-glycosidic linkages between the sugars units in hemicellulose

*ν = stretching; δ = bending; d = deformation.

vibration mode of the hydroxyl group (OH–) of carbohydrates and absorbed water. The bands observed at 2923 and 2857 cm^{-1} can be attributed to the presence of symmetric and asymmetric aliphatic C – H stretching, respectively, in the structure of lignin, cellulose, and hemicellulose. The shoulder at 1711 cm^{-1} and the absorption bands at 1603 and 1515 cm^{-1} are assigned to C=O stretching vibration of carboxylic acid in lignin and ester group in hemicellulose C=C aromatic ring, and aromatic skeletal vibrations of lignin. Respectively. Moreover, bands at 1424 and 1380 cm^{-1} were due to CH in-plane deformation of lignin and CH bending bonds of carbohydrates (hemicellulose and cellulose). In the carbohydrate fingerprint region (1290 to 850 cm^{-1}), bands at 1247 (C–O and O–H in plane stretching in hemicellulose), 1055 (C–OH stretching of cellulose), 1152 (C–O–C asymmetric stretching in cellulose and hemicellulose), 1028 (C–H deformation in cellulose and C–O stretching in hemicellulose) and 875 cm^{-1} (β-glycosidic linkages between the sugars units in hemicellulose) highlighted the presence of hemicellulose and cellulose.

Quasi-static and dynamic mechanical properties of composites

Figure 6 shows the results of tensile tests. A modification in the ductile behavior of neat HDPE is visible with the addition of PV filler along with the occurrence of a brittle fracture when a filler amount of 20 wt.% is used (Figure 6a). The highest elongation at break was observed in the case of neat HDPE (the test was interrupted before final failure) while, with the inclusion of PV filler, a reduction in HDPE ductility occurred with a slight improvement in the stiffness of the composites. The addition of PV filler did not compromise the overall mechanical properties of HDPE matrix (Figure 6b–c) despite the absence of any strategy aimed at increasing the filler/matrix interfacial adhesion.

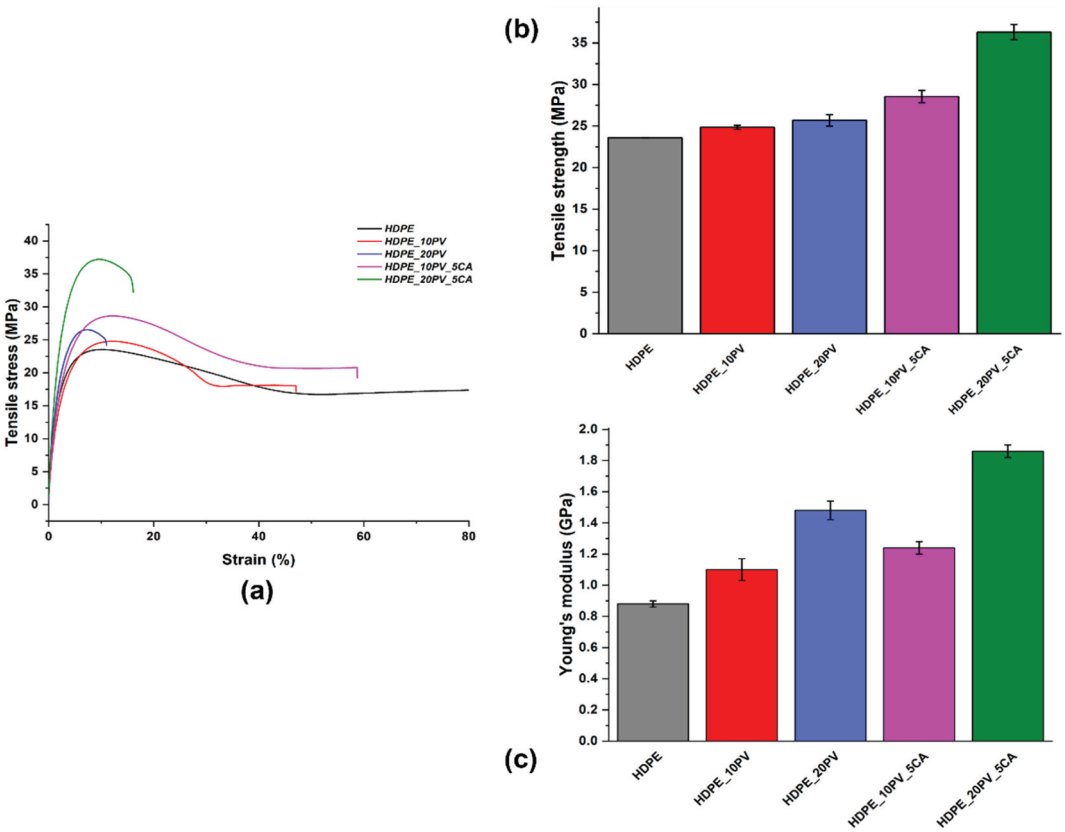

Figure 6. (a) Tensile stress – strain curves, (b) tensile strength and (c) Young's modulus of neat HDPE and biocomposites.

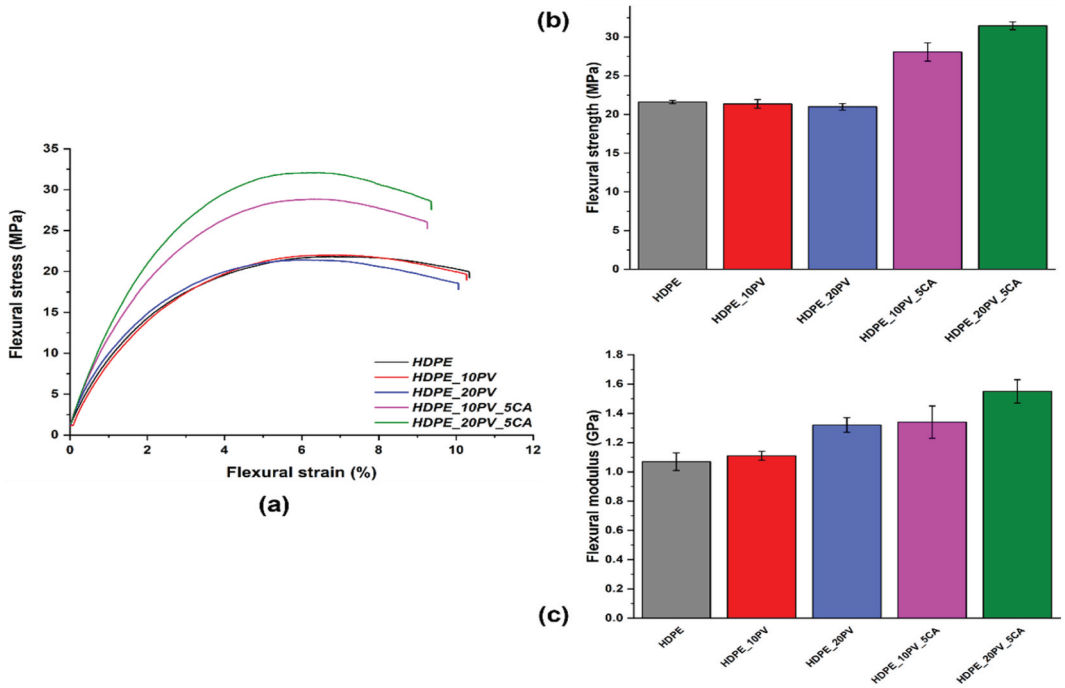

Figure 7. (a) Flexural stress – strain curves, (b) flexural strength and (c) flexural modulus of HDPE and biocomposites.

The same evidence was collected during the flexural tests (Figure 7): the addition of PV filler at the adopted amount (10 wt.% and 20 wt.%) proved to be irrelevant to flexural stress–strain curves (**Figure 7a**) and to flexural properties (Figure 7b–c). The increase in the tensile and flexural moduli is typical of composites where a rigid filler is added into a thermoplastic matrix (Haque et al. 2010). These results are in line with other works: for instance, Adhikary et al. tested wood-plastic composites based on HDPE and *Pinus radiata* as filler and in both tensile and flexural properties recorded a decrease in the strength and an increase in the modulus of elasticity at increasing wood content (Adhikary, Pang, and Staiger 2008). Kilinic and coworkers pointed-out the influence of filler agglomeration on mechanical properties with a reduction in the tensile strength up to 16.20 MPa when 20 wt. % vine stem filler was added to a HDPE matrix (Kilinc et al. 2016). These results are in contrast to other researches where lignocellulosic fillers enhanced the mechanical properties (Agayev and Ozdemir, 2019; Bavasso et al. 2020; Başboğa et al. 2020; Dolçà et al. 2022) and this is because, as mentioned in the introduction section and from XRD analysis (Figure 4a), even if PV contains cellulose (~40 wt.%), hemicellulose (~7 wt.%) and lignin (~28 wt.%) (Jiang et al. 2020), it is also rich in bio-active compounds such as polyphenols and organic acids that might reduce the compatibility with the matrix as a consequence of their hydrophilic nature (Cai et al. 2021).

The addition of a commercially available CA in the composite formulation was tested and this proved to be effective in enhancing both tensile and flexural properties with respect to the neat HDPE and non-compatibilized specimens (Figures 6and 7). In the case of 10 wt.% of PV, this improvement reached 20.9% for the tensile strength, 40.9% for the Young's modulus, 29.9% for the flexural strength, and 23.4% for the flexural modulus. When a 20 wt.% of PV was added to the composite formulation, such enhancements were 53.8% for the tensile strength, 100% for the Young's modulus, 45.6% for the flexural strength and 44.9% for the flexural modulus. This is due to the well-known action of the CA that improves the adhesion between the hydrophilic filler and the hydrophobic matrix through the ester linkages among hydrophilic OH groups and acid anhydride groups (Rao, Zhou, and Fan 2018).

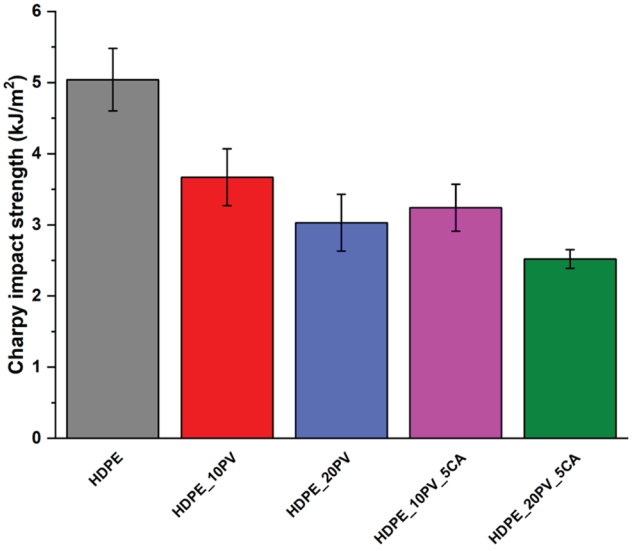

Figure 8. Charpy impact strength test results of HDPE and biocomposites.

The results of the Charpy impact tests are reported in Figure 8 where the addition of a PV filler content up to 20 wt.% and the presence of the CA were not sufficient to improve the impact strength of the biocomposites with respect to the neat HDPE specimens. The increase in the filler amount contributed to enhancing the particle–particle contact that affects the failure (Fletes and Rodrigue 2021). The presence of the PV filler can promote stress concentrations at filler ends in addition to reducing the polymer chain mobility and the ability to absorb energy during fracture propagation (Nygård et al. 2008; Ashori and Nourbakhsh 2010). This effect is even more pronounced with increasing interfacial adhesion through CA addition, thus prompting a significant reduction in impact strength. Crack propagation can be also hindered by energy absorption due to filler fracture, which is not expected to be relevant in the present case due to the limited cellulose amount in PV (~40 wt.%). However, the values of flexural strength can be considered higher with respect to requirements for applications such as lumber decking boards with a required minimum flexural strength of about 6.9 MPa (Başboğa et al. 2020).

These results are supported by SEM micrographs of fractured surfaces (Figure 9): without CA (Figure 9c–e), filler pull-out and debonding phenomena with clean lateral surfaces are visible. It is possible to observe the presence of gaps between the matrix and the filler (red arrow in Figure 9c–e), thus suggesting a non-optimal interfacial adhesion resulting in poor tensile and flexural strength values compared to neat HDPE and non-compatibilized formulations (Figures 6b and 7b). An overall brittle behavior is noted at the macroscale, with only limited ductility down to the microscale (this is related to the polymer matrix how supported by Figure 9a,b), thus confirming the macroscopic trends observed during tensile and flexural tests (**Figures 6a** and **7a**). It is possible to observe a modification in PV morphology with respect to the filler prior to the composite manufacturing (Figure 2): although the tubular structure is maintained, the grooved structure is partially lost and the pores seem more compressed in the composite formulation. The use of the compatibilizing agent clearly improved the interfacial adhesion, by reducing the pull-out length of the filler, which was fractured mainly on the same plane of the composite. It is also worth noting the absence of debonding at the filler/matrix interface, with fillers well embedded in the polymer matrix (Figure 9d–f). The enhanced interfacial adhesion supports the improved mechanical properties featured by compatibilized formulations (**Figures 6b** and **7b**) (Kabir et al. 2012; Keener, Stuart, and Brown 2004). It is also evident the progressive brittle behavior of the fracture surface, which is associated with the hindered mobility of

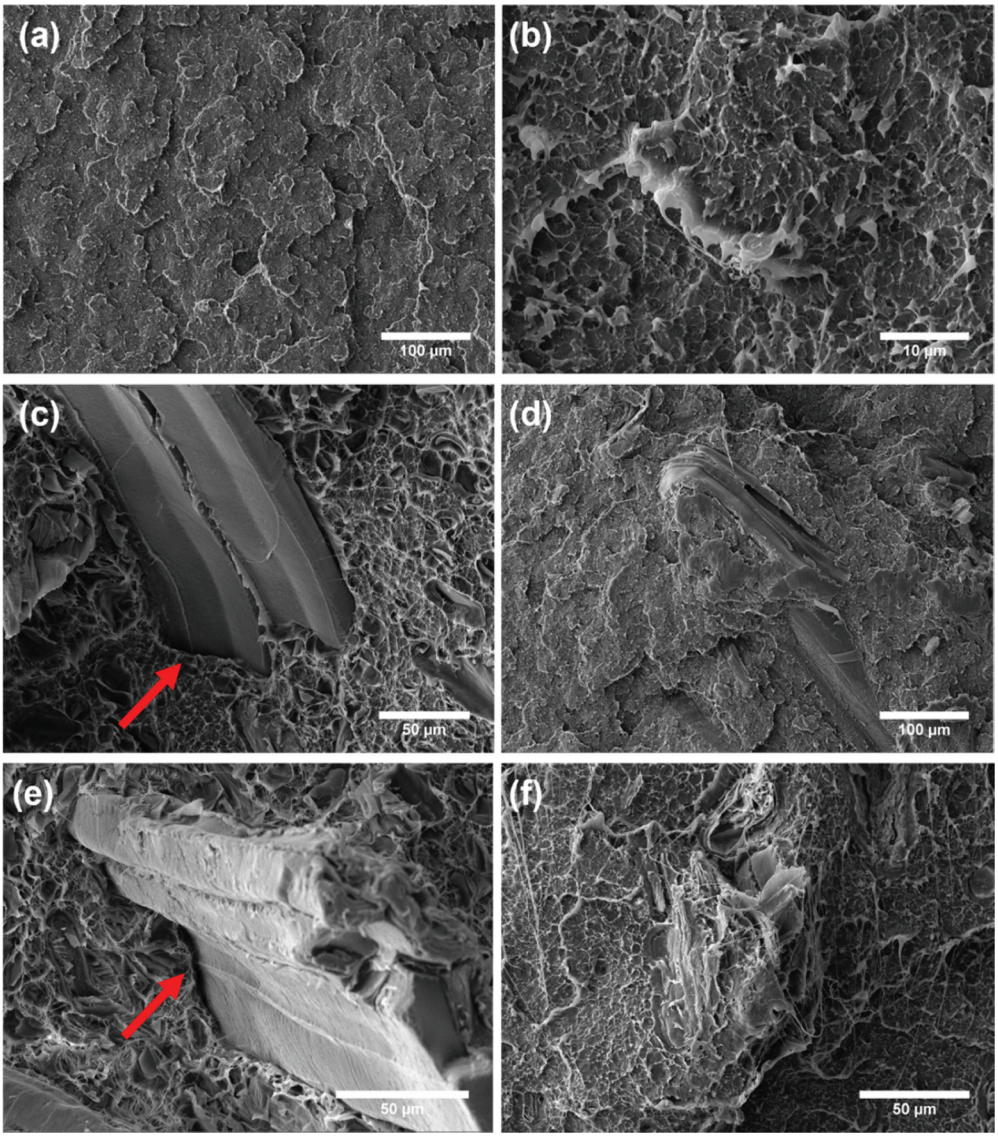

Figure 9. SEM micrographs of the fracture surfaces of (a,b) neat HDPE, (c) HDPE_10PV, (d) HDPE_10PV_5CA, (e) HDPE_20PV and (f) HDPE_20PV_5CA.

HDPE segments with increasing filler content and interfacial adhesion, resulting in poor impact strength as reported in Figure 8.

In order to assess the potential of PV root fibers in composite applications, the tensile and flexural properties of the developed composites were benchmarked against those from other studies on HDPE reinforced with waste and residues from the industrial and agricultural processes, which are still underutilized as low-value energy sources (Table 3). In general, considering the obvious differences related to fiber lengths, processing conditions, fiber content, type and amount of compatibilizing agent, the mechanical properties are comparable with those of other studies, thus confirming the potential of such organic residue (PV) to produce natural fiber composites that represent an ecologically friendly and a substantially higher value alternative to common waste management methods, including landfilling, composting, or anaerobic digestion.

Table 3. Summary of mechanical properties of polymer matrix composites reinforced with natural fibers.

Matrix type	Fibre type	Coupling agent	Tensile modulus (GPa)	Tensile strength (MPa)	Flexural strength (MPa)	Flexural modulus (GPa)	Fibre content (wt %)	Reference
HDPE	P.Vittata	yes	1.9	36.3	31.4	1.5	20	This work
HDPE	P.Vittata	no	1.5	25.7	20.9	1.3	20	This work
HDPE	Hemp	yes	3.8	36.0	-	-	30	(Sergi et al. 2019)
HDPE	Flax	no	4.6	21.6	43.6	5.1	40	(Mazur et al. 2020)
HDPE	Moso bamboo	yes	4.7	29.5	52.5	5.3	60	(Zheljazkov, Callahan, and Cantrell 2008)
HDPE	wheat straw	yes	4.5	26.3	44.5	4.8	60	(Zheljazkov, Callahan, and Cantrell 2008)
HDPE	rice straw	yes	3.4	22.5	45.0	4.3	60	(Zheljazkov, Callahan, and Cantrell 2008)
HDPE	rice husk	yes	3.0	21.0	39.2	3.2	60	(Zheljazkov, Callahan, and Cantrell 2008)
HDPE	sugarcane bagasse	yes	3.4	23.5	48.0	4.1	60	(Zheljazkov, Callahan, and Cantrell 2008)
HDPE	cotton stalk	yes	3.6	26.5	48.1	4.3	60	(Zheljazkov, Callahan, and Cantrell 2008)
HDPE	wheat straw	no	3.1	20.8	39.9	3.9	65	(Panthapulakkal and Sain 2007)
HDPE	wheat straw	yes	3.2	25.7	47.5	4.0	65	(Panthapulakkal and Sain 2007)
HDPE	corn stem	no	2.1	16.4	32.5	2.2	65	(Panthapulakkal and Sain 2007)
HDPE	corn stem	yes	1.9	19.4	34.0	2.0	65	(Panthapulakkal and Sain 2007)
HDPE	corn cob	no	1.3	10.8	25.6	1.3	65	(Panthapulakkal and Sain 2007)
HDPE	corn cob	yes	1.3	12.4	30.0	1.5	65	(Panthapulakkal and Sain 2007)
HDPE	wood flour	no	2.6	15.6	32.6	2.6	65	(Panthapulakkal and Sain 2007)
HDPE	wood flour	yes	2.5	18.6	37.1	2.7	65	(Panthapulakkal and Sain 2007)
HDPE	hemp pomace	no	1.4	17.6	-	-	30	(Merkel et al. 2014)
HDPE	hemp pomace	yes	1.7	21.6	-	-	30	(Merkel et al. 2014)
HDPE	hemp straw	no	1.8	18.7	-	-	30	(Merkel et al. 2014)
HDPE	hemp straw	yes	2.2	24.7	-	-	30	(Merkel et al. 2014)
HDPE	linseed cake	no	0.7	17.5	-	-	20	(Barczewski, Mysiukiewicz, and Kloziński 2018)

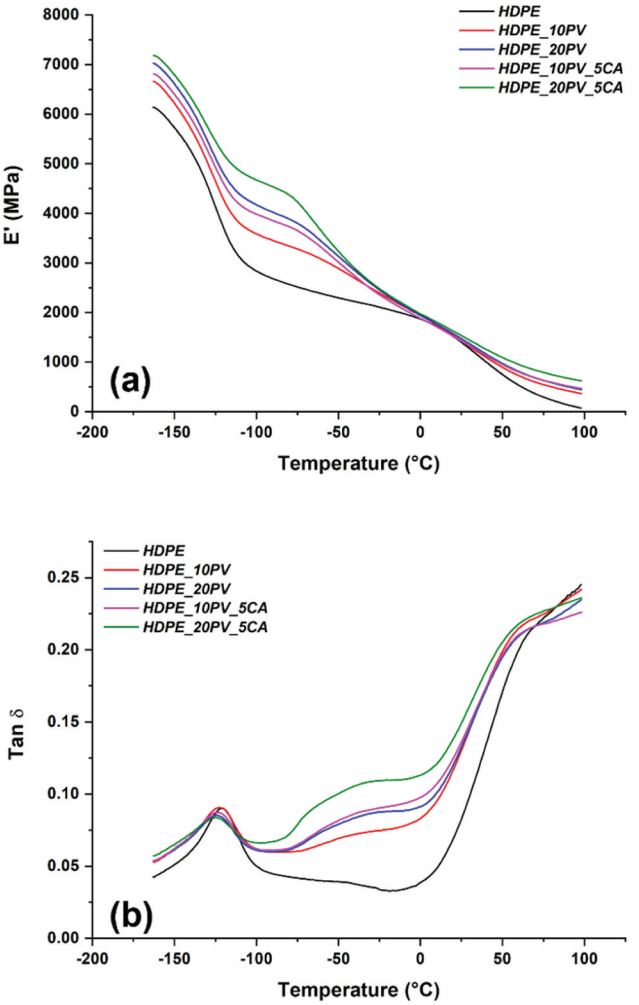

Figure 10. (a) Storage modulus (E′) and (b) damping factor (Tanδ) for neat HDPE and biocomposites.

Table 4. Storage Modulus (E′), glass transition temperature (T_g) and damping factor (Tanδ) at T_g of HDPE and biocomposites.

Sample	*E′ (MPa) at -145 ℃*	*E′ (MPa) at -100 ℃*	*E′ (MPa) at -75 ℃*	*E′ (MPa) at 25 ℃*	*T_g (℃)*	*Tanδ at T_g*
HDPE	5514.5	2836.0	2514.5	1377.3	−125.0	8.6×10^{-2}
HDPE_10PV	6020.6	3597.4	3289.6	1421.8	−128.8	8.4×10^{-2}
HDPE_10PV_5CA	6206.6	3993.0	3661.5	1419.4	−129.7	8.1×10^{-2}
HDPE_20PV	6424.6	4188.0	3816.4	1469.7	−131.9	8.2×10^{-2}
HDPE_20PV_5CA	6615.7	4683.7	4258.1	1532.4	−132.8	7.4×10^{-2}

The dynamic mechanical properties of the biocomposites were investigated by Dynamic Mechanical Analysis (DMA) whose results are reported as storage modulus (E;' Figure 10a) and dynamic damping factor (Tanδ; Figure 10b). According to literature, the addition of the filler on the composite formulations produced an enhancement of the E' (Figure 10a) with respect to the neat HDPE because the PV filler acted as a mechanical restraint (Sewda and Maiti 2013) on macromolecules mobility with a corresponding increase in stiffness of the biocomposites (Dolçà et al. 2022), in agreement with the results from the quasi-static mechanical tests. This difference is gradually

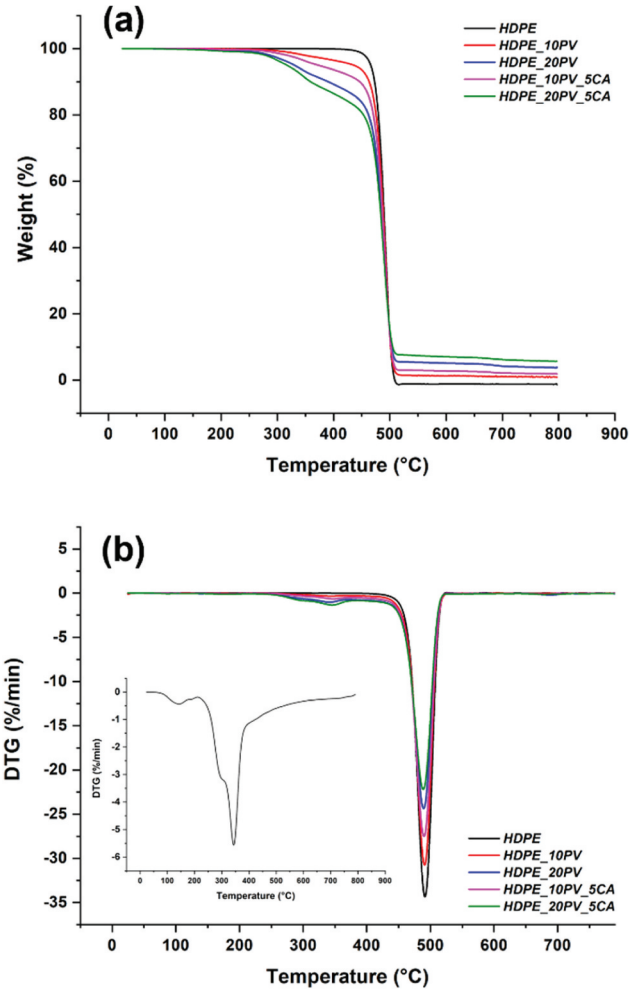

Figure 11. (a) TG and (b) DTG curves (with DTG of PV as inset) of neat HDPE and biocomposites.

smoothed out as the temperature increases, where the effect of the polymer softening predominates. The storage modulus values are summarized in Table 4 where it is possible to notice the increase in E' with the increase of PV amount in the glassy (−145°C), leathery (−100°C), rubbery plateau (−75°C) and room temperature (25°C) regions. Such trend is in line with the flexural moduli trend previously discussed and with other works, where the addition of the filler contributed to the stress transfer from the matrix to the reinforcing material (Dolçà et al. 2022; Salleh et al. 2014) and the CA positively improved the adhesion between matrix and filler with a resulting increase in the storage modulus value (Mohanty, Verma, and Nayak 2006).

In Table 4, the decreasing trend of T_g (evaluated as the peak of Tanδ), even if to a small extent, suggests the absence of a significant hindrance effect of PV filler on polymer chain mobility and the occurrence of a non-aided nucleation mechanism, leading to the formation of less perfect crystals (supported by the results on the degree of crystallinity which will be discussed in the section on DSC). The presence of the CA, as a low molecular weight polymer, promoted the polymer ability to move more freely acting as plasticizer (Tajvidi, Falk, and Hermanson 2006). The slight decrease in the damping factor (Table 4) is due to the increase in the filler amount that leads to a rigid system (Gironès et al. 2012) and to the presence of the CA which reduces the frictional damping at the filler-matrix interphase (Gil-Castell et al. 2016; Etaati et al. 2014).

Table 5. Results of DSC analysis of neat HDPE and biocomposites.

Sample	*Tc* (°C)	*Tm* (°C)	*ΔHm* (J/g)	*Xc* (%)
HDPE	115.4 ± 0.2	139.3 ± 0.3	228.6 ± 3.5	78.4 ± 0.9
HDPE_10PV	115.1 ± 0.2	137.5 ± 0.2	202.6 ± 2.8	76.8 ± 0.7
HDPE_10PV_5CA	115.2 ± 0.3	134.9 ± 0.2	165.7 ± 3.6	70.2 ± 0.7
HDPE_20PV	115.1 ± 0.1	135.7 ± 0.3	190.8 ± 3.2	72.5 ± 0.8
HDPE_20PV_5CA	115.6 ± 0.2	134.3 ± 0.2	159.0 ± 3.3	67.9 ± 0.9

Thermal properties of composites

TGA and DTG curves of HDPE_PV composites are reported in Figure 11. The maximum decomposition temperature of the PV (inset in Figure 11b) of about 345.5°C highlights good thermal stability of the filler and similar to that of other plant materials, such as pineapple leaf fiber (~366°C) (Jain, Jain, and Sinha 2019), *Passiflora foetida* steam (~383°C) (Natarajan, Kumaravel, and Palanivelu 2016), Eucalyptus (~347°C) (Carrillo et al. 2018). However, from a single thermal degradation stage typical of the neat HDPE (Figure 11b), with a maximum thermal degradation temperature of about 491.5°C (Başboğa et al. 2020), a two-stage degradation profile was obtained when the PV filler was added. The early onset of thermal decomposition range between 200°C and 375°C can be ascribed to the degradation of hemicellulose and cellulose constituents (Leszczyńska et al. 2021) of PV. The reduction in thermal stability is highlighted by the decrease in the initial onset temperature values (calculated as the temperature corresponding to a weight loss of 5%) equal to 466.1°C for HDPE, 435.8°C for HDPE_10PV, 330.5°C for HDPE_20PV, 373.1°C for HDPE_10PV_5CA and 317.2°C for HDPE_20PV_5CA. Such trend was observed elsewhere (Gil-Castell et al. 2016) and, apart from the decrease in thermal stability due to the addition of the filler, the further reduction provided by the CA was pointed out as a result of its action as dispersing agent when adopted at high concentration (El-Sabbagh 2014), which was not optimized in the present study. The mass residue at 600°C was negligible for HDPE specimens and up to 6.2% in the formulation of HDPE_20PV_5CA as a result of the delay in HDPE decomposition due to char production from PV filler (Araújo, Waldman, and De Paoli 2008).

In Table 5 are listed the DSC characteristics of HDPE and HDPE_PV composites with and without the addition of the CA. The crystallization (T_c) and the melting (T_m) temperatures did not change significantly with the addition of PV filler and CA, which are in the range of other works (Dolçà et al. 2022). Conversely, the melting enthalpy (ΔH_m) and the crystallinity degree ($\times_c$) are influenced by the presence of PV filler (Lin et al. 2018). The presence of imperfections in the crystalline structures is due to the mechanical restraints conferred to HDPE chains as supported by DMA results previously discussed. The findings collected by Sveda and Mainiti support this evidence: they developed biocomposites based on HDPE/Teak Wood Flour that exhibited a decreasing trend of the ΔH_m and a reduction of the crystallinity degree from 65.0% (neat HDPE) to 58.6% when a maximum volume fraction of filler of about 0.32 was added (Sewda and Maiti 2010). Dolca et al. recorded a decrease in crystallinity degree from 68.9% (neat HDPE) to 59.6% with the addition of 20 wt.% of hemp fiber highlighting the role of the filler as diluting agent in the biocomposites formulations (reduction of polymer chain amount that undergoes the thermodynamic transition) (Dolçà et al. 2022). The CA contributes to lower the crystallinity level because of the enhancement of interfacial bonding strength between the filler and the matrix (Dolçà et al. 2022; Sewda and Maiti 2010; Ding et al. 2021). Satapathy and Kothapalli (Satapathy and Kothapalli 2018), similarly to Lei et al. (2007), highlighted the role of maleic anhydride in the reduction of perfection of HDPE crystals.

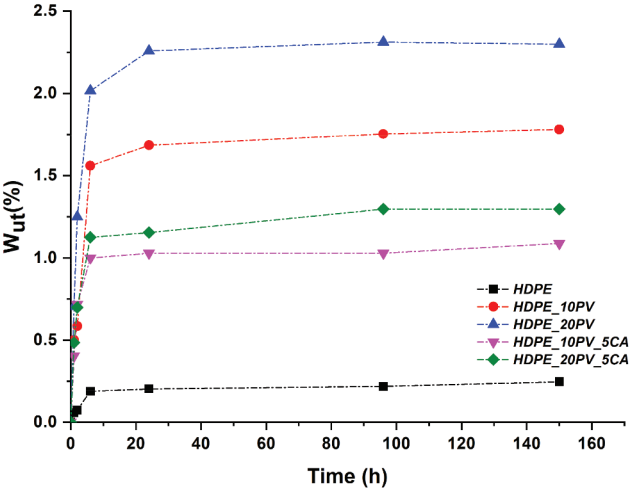

Figure 12. Water uptake as a function of time of neat HDPE and biocomposites.

Table 6. Equilibrium water uptake (W_{ut}) and estimated parameters for diffusion coefficient (D) kinetic coefficients (k and n).

Sample	W_{ut} (%)	D (cm^2/s)	k (h^2)	n(-)
HDPE	0.25		0.23	0.32
HDPE_10PV	1.78		0.25	0.66
HDPE_10PV_5CA	1.09	2.74×10^{-3}	0.40	0.49
HDPE_20PV	2.29		0.33	0.57
HDPE_20PV_5CA	1.30	2.32×10^{-3}	0.38	0.47

Water uptake of composites

Biocomposites have a high tendency to absorb water with respect to the neat polymer, due to the presence of hydrophilic groups and, in particular, when lignocellulosic compounds are added as filler (Dolçà et al. 2022; Zhuo et al. 2019). The tested biocomposites showed a constant value of the W_{ut} after 5 days of immersion in water (Figure 12): after an initial increase in moisture absorption trend in all materials, a saturation condition was reached after 24 h of immersion in water for HDPE_10PV and HDPE_20PV. In case of neat HDPE and biocomposites with the CA, the saturation condition was observed after 6 h. All results were used for the evaluation of absorption kinetic by Equation 3 and its linearization (Equation 4) (Bazan et al. 2020):

$$\frac{M(t)}{M_m} = kt^n \tag{3}$$

$$\log\left(\frac{M(t)}{M_m}\right) = \log(k) + n\log(t) \tag{4}$$

where $M_{(t)}$ and M_m are the moisture content at a specific time (t) and at the equilibrium, respectively. The kinetic coefficient k identifies the intercept of the curve while the value of the slope (n) gives information about the absorption mechanism. How it is possible to observe in Table 6, the absorption of water increased from 0.25% (neat HDPE) to 2.29% (HDPE_20PV), due to the presence of PV (which has an absorption of water equal to 1.84% and 2.75% for the same amount of dried PV in the HDPE_10PV and HDPE_20PV, respectively), and the extent of the increase of such value was similar to other works: Kilinc and collaborators measured

a W_{ut} of about 0.5% after 100 h in HDPE composites with a filler content of about 10 wt.% (35 wt.% of cellulose) (Kilinc et al. 2016), while Espert et al. reported a W_{ut} close to 6.5% for polypropylene-based composites with a 30 wt.% sisal filler (50 wt.% of cellulose) (Espert, Vilaplana, and Karlsson 2004) after the same immersion time. For the specimens HDPE_10PV and HDPE_20PV, the calculated *n* value revealed Non-Fick or anomalous diffusion (Bazan et al. 2020) and the absorption of water is mainly attributable to surface microcracks of the polymer and poor fiber/matrix adhesion, thus resulting mainly in a capillary diffusion (Le Duigou, Davies, and Baley 2009). CA confirmed its role as a compatibilizer, leading to a reduced water absorption, which was higher with respect to HDPE but reduced of about 38.9% (HDPE_10PV_5CA) and 43.6% (HDPE_20PV_5CA) compared to the same formulations without CA. This behavior can be ascribed to the reaction of maleic anhydride with free hydrophilic oxygen-based groups thus decreasing the water absorption and swelling of the filler (Patil et al. 2000).

Only for HDPE_10PV_5CA and HDPE_20PV_5CA the calculated *n* values were close to 0.5 (Table 4) suggesting the occurrence of a Fickian diffusion mechanism (Bazan et al. 2020) and it was possible to estimate the diffusion coefficient (D) by Equation 5:

$$D = \pi\left(\frac{kh}{4M_m}\right)^2 \tag{5}$$

where k and M_m are the kinetic coefficient and the moisture content at the equilibrium, respectively, while h is the thickness of the specimens. The calculated values showed that the saturation condition is reached with an almost similar initial trend (same slope of the linear region) showing diffusion values very close to each other (Moudood et al. 2019).

Conclusions

Composites of HDPE and *Pteris vittata* waste root fibers were successfully produced, via extrusion and injection molding, with up to 20 wt% fiber content with and without a commercial-maleated coupling agent. This work presents the first study, to our knowledge, on investigating the *Pteris vittata* root fiber properties and the mechanical performance of its resulting composites. These waste fibers featured a thermal stability in line with other lignocellulosic natural fibers, though characterized by a low amount of cellulose with limited crystallinity. A significant residue at the end of thermogravimetric analysis was ascribed to the presence of minerals in the water used for their growth. The addition of the filler did not degrade the tensile and flexural strengths compared to neat HDPE, while the stiffness was improved. The results of DMA and DSC analyses pointed out a hindrance effect of PV filler on polymer chain mobility and the occurrence of a non-aided nucleation mechanism. The coupling agent proved to be effective in mechanical properties enhancement, because of the improvement of the filler/matrix adhesion, as confirmed by SEM analysis. Nonetheless, it contributed to lower the crystallinity degree of the resulting biocomposites and the water absorption attitude, because of the reduction in gaps at the polymer/filler interface and the availability of free hydrophilic oxygen groups on filler's surface. The overall thermal stability was reduced by the presence of the filler and by the addition of the CA, which likely acted as dispersing agent, being its amount not optimized in the formulations investigated. In summary, without any specific refining and pre-treatment of the filler, the *Pteris vittata* root fiber demonstrated its significant potential as a valuable fiber source for polymer composites. Future research is directed toward surface modification strategies with a view to further improving the mechanical properties of PV composites for broader engineering applications.

Highlights

- High-density polyethylene (HDPE)-based biocomposites reinforced with *Pteris vittata* waste roots were manufactured.
- Two different filler amounts (10 wt.% and 20 wt.%) were used and the addition of the coupling agent on biocomposites formulation was evaluated.
- An improvement in mechanical properties was promoted by the presence of the filler with the addition of the coupling agent.
- A decrease in thermal stability was promoted by the presence of the filler and by the addition of the coupling agent.
- The presence of the filler contributed to enhance the water absorption of the biocomposites.

Disclosure statement

No potential conflict of interest was reported by the author(s).

Funding

The author(s) reported there is no funding associated with the work featured in this article.

Ethical approval

This material is the authors' own original work, which has not been previously published or currently being considered for publication elsewhere. All authors have been personally and actively involved in substantial work leading to the paper, and will take public responsibility for its content.

We confirm that all the research meets ethical guidelines and adheres to the legal requirements of the study country.

References

Adhikary, K. B., S. Pang, and M. P. Staiger. 2008. Dimensional stability and mechanical behaviour of wood–plastic composites based on recycled and virgin high-density polyethylene (HDPE). *Composites Part B: Engineering* 39 (5):807–15. doi:10.1016/J.COMPOSITESB.2007.10.005.

Agayev, S., and O. Ozdemir. 2019. Fabrication of high density polyethylene composites reinforced with pine cone powder: Mechanical and low velocity impact performances. *Materials Research Express* 6 (4):045312. doi:https://doi.org/10.1088/2053-1591/aafc42.

An, Z. Z., Z. C. Huang, M. Lei, X. Y. Liao, Y. M. Zheng, and T. B. Chen. 2006. Zinc tolerance and accumulation in Pteris Vittata L. and its potential for phytoremediation of Zn- and As-contaminated soil. *Chemosphere* 62 (5):796–802. doi:10.1016/j.chemosphere.2005.04.084.

Antenozio, L. M., G. Capobianco, P. Costantino, T. Vamerali, G. Bonifazi, S. Serranti, P. Brunetti, and M. Cardarelli. 2022. Arsenic accumulation in Pteris Vittata : Time course, distribution, and arsenic-related gene expression in fronds and whole plantlets ☆. *Environmental Pollution* 309 (July):119773. doi:10.1016/j.envpol.2022.119773.

Antenozio, M. L., G. Giannelli, R. Marabottini, P. Brunetti, E. Allevato, D. Marzi, G. Capobianco, G. Bonifazi, S. Serranti, G. Visioli, et al. 2021. Phytoextraction efficiency of Pteris Vittata grown on a naturally as-rich soil and characterization of as-resistant rhizosphere bacteria. *Scientific Reports* 11 (1). doi: https://doi.org/10.1038/s41598-021-86076-7.

Araújo, J. R., W. R. Waldman, and M. A. De Paoli. 2008. Thermal properties of high density polyethylene composites with natural fibres: Coupling agent effect. *Polymer Degradation and Stability* 93 (10):1770–75. doi:10.1016/j.polymdegradstab.2008.07.021.

Ashori, A., and A. Nourbakhsh. 2010. Reinforced polypropylene composites: Effects of chemical compositions and particle size. *Bioresource Technology* 101 (7):2515–19. doi:10.1016/J.BIORTECH.2009.11.022.

Barczewski, M., O. Mysiukiewicz, and A. Kloziński. 2018. Complex modification effect of linseed cake as an agricultural waste filler used in high density polyethylene composites. *Iranian Polymer Journal (English Edition)* 27 (9):677–88. doi:10.1007/s13726-018-0644-3.

Barman, A., N. K. Shrivastava, B. B. Khatua, and B. C. Ray. 2015. Green composites based on high-density polyethylene and Saccharum spontaneum: Effect Of filler content on morphology, thermal, and mechanical properties. *Polymer Composites* 36 (12):2157–66. doi:10.1002/pc.23126.

Bartos, A., J. Kócs, J. Anggono, J. Móczó, and B. Pukánszky. 2021. Effect of fiber attrition, particle characteristics and interfacial adhesion on the properties of PP/Sugarcane bagasse fiber composites. *Polymer Testing* 98:107189. doi: https://doi.org/10.1016/j.polymertesting.2021.107189.

Başboğa, İ. H., İ. Atar, K. Karakuş, and F. Mengeloğlu. 2020. Determination of some technological properties of injection molded pulverized-HDPE based composites reinforced with micronized waste tire powder and red pine wood wastes. *Journal of Polymers and the Environment* 28 (6):1776–94. doi:10.1007/s10924-020-01726-7.

Bavasso, I., M. P. Bracciale, F. Sbardella, J. Tirillò, F. Sarasini, and L. Di Palma. 2020. Effect of yerba mate (Ilex Paraguariensis) residue and coupling agent on the mechanical and thermal properties of polyolefin-based composites. *Polymer Composites* 41 (1):161–73. doi:https://doi.org/10.1002/pc.25355 .

Bazan, P., D. Mierzwinski, R. Bogucki, and S. Kuciel. 2020. Bio-based polyethylene composites with natural fiber: Mechanical, thermal, and ageing properties. *Materials* 13 (11):2595. doi:10.3390/ma13112595.

Bourmaud, A., C. Morvan, and C. Baley. 2010. Importance of fiber preparation to optimize the surface and mechanical properties of unitary flax fiber. *Industrial Crops and Products* 32 (3):662–67. doi:10.1016/j.indcrop.2010.08.002.

Cai, W., T. Chen, M. Lei, and X. Wan. 2021. Effective strategy to recycle arsenic-accumulated biomass of Pteris Vittata with high benefits. *The Science of the Total Environment* 756 (February):143890. doi:10.1016/J.SCITOTENV.2020.143890.

Carlson, E. D., M. T. Krejchi, C. D. Shah, T. Terakawa, R. M. Waymouth, and G. G. Fuller. 1998. Rheological and thermal properties of elastomeric polypropylene. *Macromolecules* 31 (16):5343–51. doi:10.1021/ma971106q.

Carrier, M., A. Loppinet-Serani, C. Absalon, C. Aymonier, and M. Mench. 2012. Degradation pathways of holocellulose, lignin and α-cellulose from Pteris Vittata fronds in sub- and super critical conditions. *Biomass & Bioenergy* 43 (August):65–71. doi:10.1016/J.BIOMBIOE.2012.03.035.

Carrillo, I., R. T. Mendonça, M. Ago, and O. J. Rojas. 2018. Comparative study of cellulosic components isolated from different Eucalyptus species. *Cellulose* 25 (2):1011–29. doi:10.1007/s10570-018-1653-2.

Danh, L. T., P. Truong, R. Mammucari, and N. Foster. 2014. A critical review of the arsenic uptake mechanisms and phytoremediation potential of Pteris Vittata. *International Journal of Phytoremediation* 16 (5):429–53. doi:10.1080/15226514.2013.798613.

Ding, C., Y. Zhang, X. Di, N. Zhang, Y. Zhang, and X. Wang. 2021. High-density polyethylene composite filled with red mud: Effect of coupling agent on mechanical and thermal properties. *Environmental Technology (United Kingdom)* 43 (21):3283–94. doi:10.1080/09593330.2021.1921047.

Dolçà, C., E. Fages, E. Gonga, D. Garcia-sanoguera, R. Balart, and L. Quiles-carrillo. 2022. The effect of varying the amount of short hemp fibers on mechanical and thermal properties of wood–plastic composites from biobased polyethylene processed by injection molding. *Polymers* 14 (1):138. doi:10.3390/polym14010138.

El-Sabbagh, A. 2014. Effect of coupling agent on natural fibre in natural fibre/polypropylene composites on mechanical and thermal behaviour. *Composites Part B: Engineering* 57:126–35. doi:10.1016/j.compositesb.2013.09.047.

Espert, A., F. Vilaplana, and S. Karlsson. 2004. Comparison of water absorption in natural cellulosic fibres from wood and one-year crops in polypropylene composites and its influence on their mechanical properties. *Composites Part A: Applied Science and Manufacturing* 35 (11):1267–76. doi:10.1016/J.COMPOSITESA.2004.04.004.

Etaati, A., S. Abdanan Mehdizadeh, H. Wang, and S. Pather. 2014. Vibration damping characteristics of short hemp fibre thermoplastic composites. *Journal of Reinforced Plastics and Composites* 33 (4):330–41. doi:10.1177/0731684413512228.

Faludi, G., G. Dora, B. Imre, K. Renner, J. Mõczõ, and B. Pukánszky. 2014. PLA/Lignocellulosic fiber composites: Particle characteristics, interfacial adhesion, and failure mechanism. *Journal of Applied Polymer Science* 131 (4):1–10. doi:10.1002/app.39902.

Fayiga, A. O., L. Q. Ma, J. Santos, B. Rathinasabapathi, B. Stamps, and R. C. Littell. 2005. Effects of arsenic species and concentrations on arsenic accumulation by different fern species in a hydroponic system. *International Journal of Phytoremediation* 7 (3):231–40. doi:10.1080/16226510500215720.

Fletes, R. C. V., and D. Rodrigue. 2021. Effect of wood fiber surface treatment on the properties of recycled Hdpe/Maple fiber composites. *Journal of Composites Science* 5 (7):177. doi:10.3390/jcs5070177.

Gholampour, A., and T. Ozbakkaloglu. 2020. A review of natural fiber composites: Properties, modification and processing techniques, characterization, applications. *Journal of Materials Science* 55 (3):829–92. Springer US. doi:https://doi.org/10.1007/s10853-019-03990-y.

Gil-Castell, O., J. D. Badia, T. Kittikorn, E. Strömberg, M. Ek, S. Karlsson, and A. Ribes-Greus. 2016. Impact of hydrothermal ageing on the thermal stability, morphology and viscoelastic performance of PLA/Sisal Biocomposites. *Polymer Degradation and Stability* 132:87–96. doi:10.1016/j.polymdegradstab.2016.03.038.

Gironès, J., J. P. López, P. Mutjé, A. J. F. Carvalho, A. A. S. Curvelo, and F. Vilaseca. 2012. Natural fiber-reinforced thermoplastic starch composites obtained by melt processing. *Composites Science and Technology* 72 (7):858–63. doi:10.1016/J.COMPSCITECH.2012.02.019.

Gonzaga, M. I. S., J. A. G. Santos, and L. Q. Ma. 2008. Phytoextraction by arsenic hyperaccumulator Pteris Vittata l. from six arsenic-contaminated soils: Repeated harvests and arsenic redistribution. *Environmental Pollution* 154 (2):212–18. doi:10.1016/j.envpol.2007.10.011.

Hamilton, J. W., R. C. Kaltreider, O. V. Bajenova, M. A. Ihnat, J. McCaffrey, B. W. Turpie, E. E. Rowell, J. Oh, M. J. Nemeth, C. A. Pesce, et al. 1998. Molecular basis for effects of carcinogenic heavy metals on inducible gene expression. *Environmental Health Perspectives* 106 (SUPPL. 4):1005–15. doi:https://doi.org/10.1289/ehp.98106s41005 .

Haque, M., R. Rahman, N. Islam, M. Huque, and M. Hasan. 2010. Mechanical properties of polypropylene composites reinforced with chemically treated coir and abaca fiber. *Journal of Reinforced Plastics and Composites* 29 (15):2253–61. doi:10.1177/0731684409343324.

Huang, J. W., C. Y. Poynton, L. V. Kochian, and M. P. Elless. 2004. Phytofiltration of arsenic from drinking water using arsenic- hyperaccumulating ferns. *Environmental Science & Technology* 38 (12):3412–17. doi:10.1021/es0351645.

Jain, J., S. Jain, and S. Sinha. 2019. Characterization and thermal kinetic analysis of pineapple leaf fibers and their reinforcement in epoxy. *Journal of Elastomers and Plastics* 51 (3):224–43. doi:10.1177/0095244318783024.

Jeyabalaji, V., G. R. Kannan, P. Ganeshan, K. Raja, B. NagarajaGanesh, and P. Raju. 2021. Extraction and characterization studies of cellulose derived from the roots of Acalypha Indica L. *Journal of Natural Fibers* 19 (12):4544–56. doi:10.1080/15440478.2020.1867942.

Jiang, H., L. Fan, C. Cai, Y. Hu, F. Zhao, R. Ruan, and W. Yang. 2020. Study on the bio-oil characterization and heavy metals distribution during the aqueous phase recycling in the hydrothermal liquefaction of as-enriched Pteris Vittata L. *Bioresource Technology* 317 (December):124031. doi:10.1016/J.BIORTECH.2020.124031.

Kabir, M. M., H. Wang, K. T. Lau, and F. Cardona. 2012. Chemical treatments on plant-based natural fibre reinforced polymer composites: An overview. *Composites Part B: Engineering* 43 (7):2883–92. doi:10.1016/j.compositesb.2012.04.053.

Keener, T. J., R. K. Stuart, and T. K. Brown. 2004. Maleated coupling agents for natural fibre composites. *Composites Part A: Applied Science and Manufacturing* 35 (3):357–62. doi:10.1016/j.compositesa.2003.09.014.

Kilinc, A. C., M. Atagur, O. Ozdemir, I. Sen, N. Kucukdogan, K. Sever, O. Seydibeyoglu, M. Sarikanat, and Y. Seki. 2016. Manufacturing and characterization of vine stem reinforced high density polyethylene composites. *Composites Part B: Engineering* 91 (April):267–74. doi:10.1016/J.COMPOSITESB.2016.01.033.

Koffi, A., D. Koffi, and L. Toubal. 2021. Mechanical properties and drop-weight impact performance of injection-molded HDPE/Birch fiber composites. *Polymer Testing* 93:106956. doi: https://doi.org/10.1016/j.polymertesting.2020.106956.

Le Duigou, A., P. Davies, and C. Baley. 2009. Seawater ageing of Flax/Poly(Lactic Acid) biocomposites. *Polymer Degradation and Stability* 94 (7):1151–62. doi:10.1016/j.polymdegradstab.2009.03.025.

Lei, Y., Q. Wu, F. Yao, and Y. Xu. 2007. Preparation and properties of recycled HDPE/Natural fiber composites. *Composites Part A: Applied Science and Manufacturing* 38 (7):1664–74. doi:10.1016/j.compositesa.2007.02.001.

Leszczyńska, M., E. Malewska, J. Ryszkowska, M. Kurańska, M. Gloc, M. K. Leszczyński, and A. Prociak. 2021. Vegetable fillers and rapeseed oil-based polyol as natural raw materials for the production of rigid polyurethane foams. *Materials* 14 (7):1–22. doi:10.3390/ma14071772.

Lin, S., M. A. S. Anwer, Y. Zhou, A. Sinha, L. Carson, and H. E. Naguib. 2018. Evaluation of the thermal, mechanical and dynamic mechanical characteristics of modified graphite nanoplatelets and graphene oxide high-density polyethylene composites. *Composites Part B: Engineering* 132:61–68. doi:10.1016/j.compositesb.2017.08.010.

Ma, L. Q., K. M. Komar, C. Tu, W. Zhang, Y. Cai, and E. D. Kennelley. 2001. A fern that hyperaccumulates arsenic. *Nature* 409 (6820):579. doi:10.1038/35054664.

Marzi, D., M. L. Antenozio, S. Vernazzaro, C. Sette, E. Veschetti, L. Lucentini, G. Daniele, P. Brunetti, and M. Cardarelli. 2021. Advanced drinking groundwater as phytofiltration by the hyperaccumulating fern Pteris Vittata. *Water (Switzerland)* 13 (16):2187. doi:https://doi.org/10.3390/w13162187.

Mazur, K., P. Jakubowska, P. Romańska, and S. Kuciel. 2020. Green high density polyethylene (HDPE) reinforced with basalt fiber and agricultural fillers for technical applications. *Composites Part B: Engineering* 202:108399. doi:10.1016/j.compositesb.2020.108399.

Mazzeo, L., D. Marzi, I. Bavasso, M. Paola, V. Piemonte, and L. Di. 2022. Characterization of waste roots from the as hyperaccumulator Pteris Vittata as low-cost adsorbent for methylene blue removal. *Chemical Engineering Research & Design* 186:13–21. doi:10.1016/j.cherd.2022.07.025.

Merkel, K., H. Rydarowski, J. Kazimierczak, and A. Bloda. 2014. Processing and characterization of reinforced polyethylene composites made with lignocellulosic fibres isolated from waste plant biomass such as hemp. *Composites Part B: Engineering* 67:138–44. doi:10.1016/j.compositesb.2014.06.007.

Mohanty, S., S. K. Verma, and S. K. Nayak. 2006. Dynamic mechanical and thermal properties of MAPE treated Jute/HDPE composites. *Composites Science and Technology* 66 (3–4):538–47. doi:10.1016/j.compscitech.2005.06.014.

Moudood, A., A. Rahman, A. Öchsner, M. Islam, and G. Francucci. 2019. Flax fiber and its composites: An overview of water and moisture absorption impact on their performance. *Journal of Reinforced Plastics and Composites* 38 (7):323–39. doi:10.1177/0731684418818893.

Mu, B., W. Tang, T. Liu, X. Hao, Q. Wang, and R. Ou. 2021. Comparative study of high-density polyethylene-based biocomposites reinforced with various agricultural residue fibers. *Industrial Crops and Products* 172:114053. doi: https://doi.org/10.1016/j.indcrop.2021.114053.

Natarajan, T., A. Kumaravel, and R. Palanivelu. 2016. Extraction and characterization of natural cellulosic fiber from passiflora foetida stem. *International Journal of Polymer Analysis and Characterization* 21 (6):478–85. doi:10.1080/1023666X.2016.1168636.

Natarajan, S., R. H. Stamps, L. Q. Ma, U. K. Saha, D. Hernandez, Y. Cai, and E. J. Zillioux. 2011. Phytoremediation of arsenic-contaminated groundwater using arsenic hyperaccumulator Pteris Vittata L.: Effects of frond harvesting

regimes and arsenic levels in refill water. *Journal of Hazardous Materials* 185 (2–3):983–89. doi:10.1016/j.jhazmat.2010.10.002.

Nygård, P., B. S. Tanem, T. Karlsen, P. Brachet, and B. Leinsvang. 2008. Extrusion-based wood fibre–pp composites: Wood powder and pelletized wood fibres – a comparative study. *Composites Science and Technology* 68 (15–16):3418–24. doi:10.1016/J.COMPSCITECH.2008.09.029.

Panthapulakkal, S., and M. Sain. 2007. Agro-residue reinforced high-density polyethylene composites: Fiber characterization and analysis of composite properties. *Composites Part A: Applied Science and Manufacturing* 38 (6):1445–54. doi:10.1016/j.compositesa.2007.01.015.

Patil, Y. P., B. Gajre, D. Dusane, S. Chavan, and S. Mishra. 2000. Effect of maleic anhydride treatment on steam and water absorption of wood polymer composites prepared from wheat straw, cane bagasse, and teak wood sawdust using novolac as matrix. *Journal of Applied Polymer Science* 77 (13):2963–67. https://doi.org/10.1002/1097-4628(20000923)77:13<2963:AID-APP20>3.0.CO;2-0.

Pilon-Smits, E. 2005. Phytoremediation. *Annual Review of Plant Biology* 56 (1):15–39. doi:https://doi.org/10.1146/annurev.arplant.56.032604.144214.

Rao, J., Y. Zhou, and M. Fan. 2018. Revealing the interface structure and bonding mechanism of coupling agent treated WPC. *Polymers* 10 (3):1–13. doi:10.3390/polym10030266.

Rasib, S. Z. M., M. Mariatti, and H. Y. Atay. 2021. Effect of waste fillers addition on properties of high-density polyethylene composites: Mechanical properties, burning rate, and water absorption. *Polymer Bulletin* 78 (12):6777–95. doi:10.1007/s00289-020-03454-3.

Salleh, F. M., A. Hassan, R. Yahya, and A. D. Azzahari. 2014. Effects of extrusion temperature on the rheological, dynamic mechanical and tensile properties of kenaf Fiber/HDPE composites. *Composites Part B: Engineering* 58 (March):259–66. doi:10.1016/J.COMPOSITESB.2013.10.068.

Satapathy, S., and R. V. S. Kothapalli. 2018. Mechanical, dynamic mechanical and thermal properties of banana Fiber/Recycled high density polyethylene biocomposites filled with flyash cenospheres. *Journal of Polymers and the Environment* 26 (1):200–13. doi:10.1007/s10924-017-0938-0.

Sergi, C., J. Tirillò, M. C. Seghini, F. Sarasini, V. Fiore, and T. Scalici. 2019. Durability of Basalt/Hemp hybrid thermoplastic composites. *Polymers* 11 (4):1–17. doi:10.3390/polym11040603.

Sewda, K., and S. N. Maiti. 2010. Crystallization and melting behavior of HDPE in HDPE/Teak wood flour composites and their correlation with mechanical properties. *Journal of Applied Polymer Science* 118:2264–75. doi:10.1002/app.30551.

Sewda, K., and S. N. Maiti. 2013. Dynamic mechanical properties of high density polyethylene and teak wood flour composites. *Polymer Bulletin* 70 (10):2657–74. doi:10.1007/s00289-013-0941-0.

Shaji, E., M. Santosh, K. V. Sarath, P. Prakash, V. Deepchand, and B. V. Divya. 2021. Arsenic contamination of groundwater: A global synopsis with focus on the Indian Peninsula. *Geoscience Frontiers* 12 (3):101079. doi:10.1016/j.gsf.2020.08.015.

Syed, M. A., and A. A. Syed. 2016. Development of green thermoplastic composites from centella spent and study of its physicomechanical, tribological, and morphological characteristics. *Journal of Thermoplastic Composite Materials* 29 (9):1297–311. doi:10.1177/0892705714563123.

Tajvidi, M., R. H. Falk, and J. C. Hermanson. 2006. Effect of natural fibers on thermal and mechanical properties of natural fiber polypropylene composites studied by dynamic mechanical analysis. *Journal of Applied Polymer Science* 101 (6):4341–49. doi:10.1002/app.24289.

Tamanna, T. A., S. A. Belal, M. A. H. Shibly, and A. N. Khan. 2021. Characterization of a new natural fiber extracted from corypha taliera fruit. *Scientific Reports* 11 (1):1–13. doi:10.1038/s41598-021-87128-8.

Vandana, U. K., A. B. M. Gulzar, L. P. Singha, A. Bhattacharjee, P. B. Mazumder, and P. Pandey. 2020. Hyperaccumulation of arsenic by Pteris Vittata, a potential strategy for phytoremediation of arsenic-contaminated soil. *Environmental Sustainability* 3 (2):169–78. doi:10.1007/s42398-020-00106-0.

Verma, R. K., M. S. Sankhla, E. B. Jadhav, K. Parihar, and K. K. Awasthi. 2022. Phytoremediation of heavy metals extracted from soil and aquatic environments: Current advances as well as emerging trends. *Biointerface Research in Applied Chemistry* 12 (4):5486–509. doi:10.33263/BRIAC124.54865509.

Xu, F., J. Yu, T. Tesso, F. Dowell, and D. Wang. 2013. Qualitative and quantitative analysis of lignocellulosic biomass using infrared techniques: A mini-review. *Applied Energy* 104:801–09. doi:10.1016/j.apenergy.2012.12.019.

Yamazaki, H., K. Ishii, S. Matsuyama, Y. Kikuchi, Y. Takahashi, Y. Kawamura, R. Watanabe, K. Tashiro, and C. Inoue. 2008. Fundamental study on an arsenic hyperaccumulator plant using Submilli-PIXE camera. *X-Ray Spectrometry* 37 (2):184–87. doi:10.1002/xrs.

Yao, F., Q. Wu, Y. Lei, W. Guo, and Y. Xu. 2008. Thermal decomposition kinetics of natural fibers: Activation energy with dynamic thermogravimetric analysis. *Polymer Degradation and Stability* 93 (1):90–98. doi:10.1016/j.polymdegradstab.2007.10.012.

Yue, Y., J. Han, G. Han, Q. Zhang, A. D. French, and Q. Wu. 2015. Characterization of cellulose I/Ii hybrid fibers isolated from energy cane bagasse during the delignification process: Morphology, crystallinity and percentage estimation. *Carbohydrate Polymers* 133:438–47. doi:10.1016/j.carbpol.2015.07.058.

Zhang, W., Y. Cai, C. Tu, and L. Q. Ma. 2002. Arsenic speciation and distribution in an arsenic hyperaccumulating plant. *The Science of the Total Environment* 300 (1–3):167–77. doi:10.1016/S0048-9697(02)00165-1.

Zhao, F. J., S. J. Dunham, and S. P. McGrath. 2002. Arsenic hyperaccumulation by different fern species. *The New Phytologist* 156 (1):27–31. doi:10.1046/j.1469-8137.2002.00493.x.

Zheljazkov, V. D., A. Callahan, and C. L. Cantrell. 2008. Yield and oil composition of 38 basil (Ocimum Basilicum L.) Accessions grown in mississippi. *Journal of Agricultural and Food Chemistry* 56 (1):241–45. doi:10.1021/jf072447y.

Zhuo, G., X. Zhang, Y. Liu, and M. Wang. 2019. Effect of multiple recycling on properties of poplar fiber reinforced high density polyethylene wood-plastic composites. *Materials Research Express* 6 (12):125514. doi:https://doi.org/10.1088/2053-1591/ab5742.